Atmospheric and Oceanic Science Letters 16 (2023) 100406

Contents lists available at ScienceDirect

Atmospheric and Oceanic Science Letters

journal homepage: www.keaipublishing.com/en/journals/atmospheric-and-oceanic-science-letters/

Can a global mean sea-level rise reduce the Last Interglacial model–data mismatch in East Asia?

Zhiqi Qian [a], Tianao Xu [b], Zhongshi Zhang [b,c,d,*], Chunju Huang [a]

[a] State Key Laboratory for Biogeology and Environmental Geology, Hubei Key Laboratory of Critical Zone Evolution, School of Earth Sciences, China University of Geosciences, Wuhan, China
[b] Department of Atmospheric Science, School of Environmental Studies, China University of Geosciences, Wuhan, China
[c] School of Geographic Science, Nantong University, Nantong, China
[d] Centre for Severe Weather and Climate and Hydro-geological Hazards, Wuhan, China

ARTICLE INFO

Keywords:
Last Interglacial
Sea-level rise
Model–data mismatch

ABSTRACT

The Last Interglacial (LIG), with its many reconstructions and simulations, provides an ideal analog for investigating the future warmer climate. However, there has been a persistent mismatch between simulated and reconstructed LIG climates in East Asia, with simulations generally indicating a colder and drier climate than reconstructions. In this study, utilizing the Norwegian Earth System Model (NorESM1-F), the authors investigated whether incorporating the global mean sea-level rise in LIG simulation experiments can reduce the model–data mismatch. The new experiments reveal a discernible, yet insufficient, warming and wetting effect in East Asia resulting from the sea-level rise. Therefore, the model–data mismatch remains unresolved. Based on these results, the authors explore alternative factors that may contribute to this mismatch, offering insights for future studies.

关键词:
末次间冰期
海平面上升
模式–数据不匹配

摘 要

末次间冰期有着丰富的重建和模拟资料, 为研究未来温暖气候提供了一个理想的参考. 然而, 关于 末次间冰期的东亚气候, 模拟与重建的结果间长期存在着不匹配的情况, 模拟结果普遍较重建结 果更为冷干. 本研究利用挪威地球系统模式(NorESM1-F), 探讨了在末次间冰期模拟试验中纳入全 球平均海平面上升能否减少模式–数据的不匹配. 该试验结果表明, 海平面上升情况下东亚地区会 产生一定的增温增湿效应, 但不足以消除模式–数据不匹配. 基于这些结果, 作者探讨了其它可能 造成不匹配的因素以供进一步研究.

1. Introduction

The Last Interglacial (LIG), which occurred between 129 and 116 ka, also known as the Eemian or MIS5e, was one of the warmest periods since the middle Pleistocene (Past Interglacials Working Group of PAGES, 2016; Hoffman et al., 2017; Turney et al., 2020). Global temperatures during the LIG are estimated to have been 0.1°C to more than 2°C higher than present-day levels (Turney et al., 2020), while the atmospheric CO_2 concentration was approximately 275 ppm (Petit et al., 1999), slightly lower than the preindustrial level. Although the naturally driven warming mechanisms during the LIG differ from the current global warming caused by greenhouse gas emissions (Pedersen et al., 2017), the LIG remains an ideal analog for investigating Earth system feedback in the future due to its relatively recent occurrence and similar geographical conditions.

In China, ice cores, loess deposits, cave stalagmites, pollen, lakes, and deep-sea sediments have provided rich records of the environment of the LIG (Table 1). Although there are some differences among these records, most indicate a warmer and more humid climate during the LIG (Leng et al., 2019). However, results from phase 4 of the Paleoclimate Modeling Intercomparison Project (PMIP4) multimodel ensemble exhibit colder and drier conditions compared to reconstructions, highlighting a model–data mismatch (Otto-Bliesner et al., 2020, 2021; Jiang et al., 2022). These PMIP4 LIG simulations overall reveal the effects of

* Corresponding author.
E-mail address: zhongshi.zhang@cug.edu.cn (Z. Zhang).

https://doi.org/10.1016/j.aosl.2023.100406
Received 30 May 2023; Received in revised form 14 July 2023; Accepted 27 July 2023
Available online 14 August 2023

Table 1
Reconstructed temperature and precipitation changes during the LIG (modified from Leng et al. (2019)).

Location	Lat. (°N)	Lon. (°E)	Proxies	Temperature	Precipitation	Reference
Guliya	35.2	81.5	Ice core	Warmer	–	Yao et al. (1997) Wu et al. (2004)
Yanchang	33.5	109.2	Loess	–	Wetter	Zhao et al. (2004)
Baoji	34.0	107.0		Warmer	Wetter	Lü et al. (1996)
Baoji	34.4	107.1		–	Wetter	Beck et al. (2018)
Xi`an	34.0	108.0		Warmer	Wetter	Guo et al. (1993)
Lantian	34.2	109.2		–	Drier	Ning et al. (2008)
Weinan	34.3	109.5		–	Wetter	Ning et al. (2008)
Weinan	34.4	109.0		Warmer	Wetter	Wen et al. (1997)
Weinan	34.4	109.5		Warmer	Wetter	Lu et al. (2007); Tang et al. (2017)
Weinan	34.5	109.0		Warmer	Wetter	Zhang (2013)
Mangshan	34.6	113.2		Warmer	–	Petersen et al. (2014)
Lingtai	35.1	107.6		Warmer	Wetter	Chen et al. (2003)
Hezuo	35.5	103.3		–	Drier	Lü (1999)
Pingliang	35.5	106.7		Warmer	Wetter	Chen et al. (2003)
Zhenyuan	35.7	107.2		Warmer	Wetter	Chen et al. (2003)
Xifeng	35.7	107.6		Warmer	Wetter	Guo et al. (1993)
Xifeng	35.7	107.7		Warmer	Drier	Chen et al. (2003)
Luochuan	35.8	109.4		Warmer	Wetter/Drier	Chen et al. (2003); Zhou et al. (2014)
Panzi Mountain	36.0	101.0		–	Wetter	Zhao et al. (2004)
Huan County	36.5	107.3		Warmer	Wetter	Chen et al. (2003)
Shagou	37.3	102.5		–	Wetter	Liu et al. (2000)
Salawusu River	37.7	108.5		Warmer	Wetter	Jin et al. (2005)
Linfen	38.0	107.0		Warmer	Wetter	Du et al. (2016)
Khorchin	43.5	121.3		–	Wetter	Zhao et al. (2004)
Tianshan Mountain	44.0	87.5		–	Wetter	Wen (2015)
Yongxing Cave	25.0	115.0	Stalagmite	–	Wetter	Jiang et al. (2008)
Dongge Cave	25.3	108.1		–	Wetter	Qin et al. (2001)
Sanbao Cave	31.4	110.3		–	Wetter	Hu et al. (2015)
Sanbao Cave	31.7	110.4		–	Wetter	Cheng et al. (2016)
Kesang Cave	43.0	82.0		–	Drier	Hu et al. (2015)
Tengchong	25.0	98.2	Lake sediment	Warmer	Wetter	Wen (2007)
Subei Basin	32.5	119.5		Warmer	–	Guo (2004)
Joergay Basin	34.0	102.4		Warmer	Wetter	Wu et al. (2000); Shen et al. (2005); Xue et al. (1999)
South China Sea (SCS)17961	6.2	112.2	Deep sea sediment	Warmer	–	Pelejero et al. (1999a, 1999b)
SCS 17954	8.5	112.3		Warmer	–	Pelejero et al. (1999a)
SCS MD97-2151	8.7	109.9		Warmer	–	Zhao et al. (2006); Yamamoto et al. (2013)
SCS MD05-2897	8.8	111.4		Warmer	–	Liang et al. (2015)
SCS ODP1143	9.5	113.2		Warmer	–	Wang et al. (2014)
SCS MD05-2901	14.4	110.7		Colder	–	Su et al. (2013)
SCS MD05-2901	14.4	110.8		Warmer	–	Li et al. (2009)
SCS V3-06-3	19.1	116.1		Warmer	–	Wang et al. (1986)
SCS MD05-2904	19.5	116.3		Warmer	–	He et al. (2008); Qiu et al. (2014)
SCS ODP1145	19.6	117.6		Warmer	–	Oppo and Sun (2005)

orbital parameters on summer warming and humidification, winter cooling and drying, and annual cooling in China.

The PMIP4 LIG experimental protocol mainly focuses on orbital parameters and greenhouse gas concentrations, without specific constraints on the global mean sea level (GMSL) (Otto-Bliesner et al., 2021). However, previous studies have shown that during the LIG, the GMSL was about 5–10 m higher than today (Fox-Kemper et al., 2021). The higher GMSL may potentially have created extensive and significant impacts on a global scale (Zhang et al., 2023). Growth of the GMSL elevates the sea-level datum (the reference surface between the topography of the land and the ocean bathymetry), leading to a deepening of ocean gateways, expansion of ocean surfaces (Farnsworth et al., 2019), a reshaping of regional relative sea levels (Church et al., 2004; Richter et al., 2020), and reorganization of ocean density structures and dynamics. Moreover, GMSL changes in the glacial–interglacial cycles exert substantial influences on global and regional climates. For instance, the opening and closing of the Bering Strait affected the Atlantic Meridional Ocean Circulation and the transport of oceanic heat (Hu et al., 2010). The landmass configuration of the Maritime Continent plays a crucial role in shaping regional atmospheric circulation and rainfall (Di Nezio et al., 2016).

Here, we further diagnose LIG snapshot experiments with the fast version of the Norwegian Earth System Model (NorESM1-F). We incorporate the GMSL rise into the LIG experiments to investigate whether considering it can reduce the long-standing model–data mismatch.

2. Model and experiments

NorESM1-F is a computationally efficient model within the Norwegian Earth System Model family that simulates the global climate well (Guo et al., 2019). It was built on the Community Climate System Model, version 4 (Gent et al., 2011). NorESM1-F utilizes a grid with a horizontal resolution of 2° and 26 vertical levels in the atmospheric component and a tripolar grid with a nominal 1° horizontal resolution and 53 vertical layers in the oceanic component. A detailed description and evaluation of NorESM1-F can be found in the model documentation by Guo et al. (2019).

In addition to the preindustrial control experiment (piControl), three

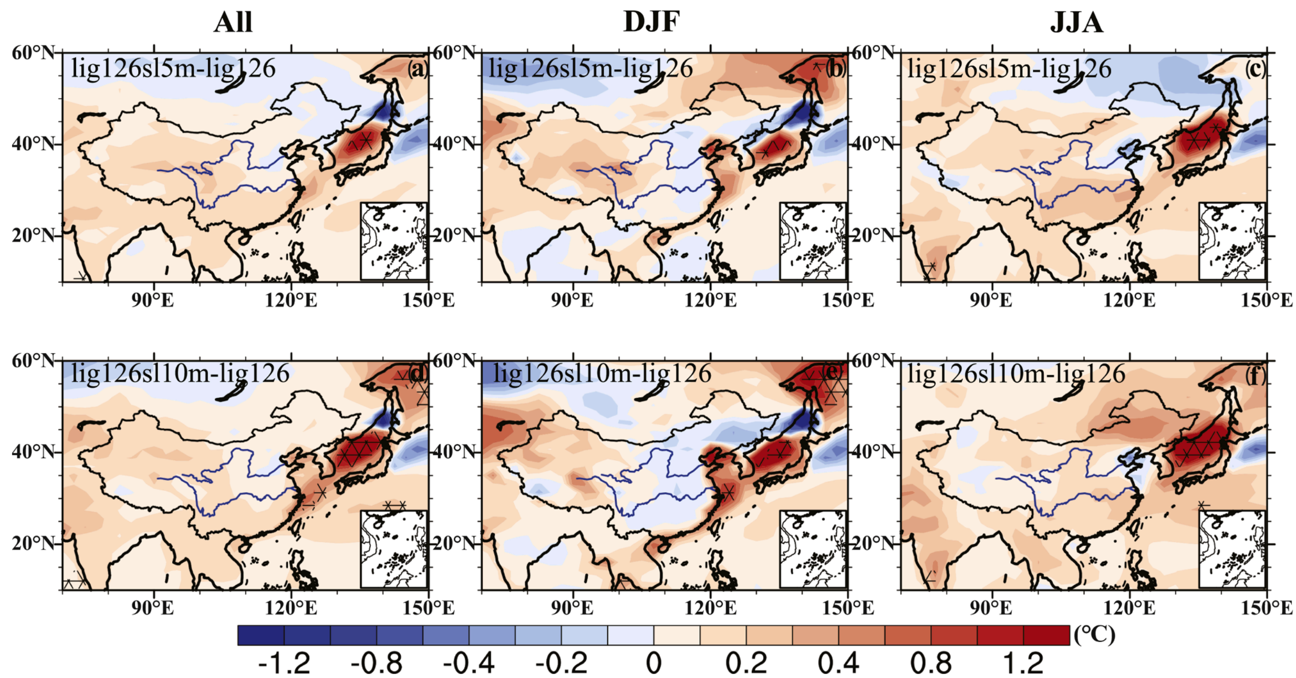

Fig. 1. Monthly temperature changes due to GMSL rise in interglacial sensitivity experiments: (a) comparison between the lig126sl5m and lig126 experiments in the response of monthly temperature (units: ℃) for the whole year; (b, c) as in (a) but in winter (DJF) and summer (JJA), respectively; (d–f) as in (a–c) but the sea-level uplifts are 10 m. The gridded area passed the 0.05 significance *t*-test.

other LIG experiments have been conducted. First, the lig126 experiment only considers changes in Earth's orbital configuration and greenhouse gas levels, using the orbital parameters of 126 ka (Berger and Loutre, 1991), an atmospheric CO_2 level of 274.99 ppm, and an atmospheric CH_4 level of 652.52 ppb (Siegenthaler et al., 2005). Subsequently, the lig126sl5m and lig126sl10m experiments incorporate additional GMSL uplifts of 5 and 10 m, respectively. In these experiments, the ocean bathymetry is adjusted by adding 5 m (10 m), while the land topography is reduced by the same amount. For a more detailed experimental design, please refer to Zhang et al. (2023).

3. Simulation results

Compared to the lig126 experiment, the lig126sl5m and lig126sl10m experiments show a slight overall increase in annual mean surface air temperature (SAT) in China, with most regions experiencing an insignificant temperature rise of less than 0.2 °C. Notably, the Japan Sea and eastern coastal areas of China exhibit a more pronounced warming, with temperature increases of up to 1 °C (Fig. 1(a, d)). This warming can be attributed to increased warm water inflow from the Northwest Pacific into the relatively enclosed Japan Sea, leading to a concentration of warm water and resulting in higher temperatures in these regions compared to the surrounding areas. The change in seasonal SAT follows a similar pattern to the annual mean SAT. In summer, apart from the Bohai Sea region, the SAT over China slightly increases (Fig. 1(b, e)). In winter, the eastern part of China experiences a slight cooling, whereas other regions show a slight warming. The significant seasonal warming is also mostly confined to the Japan Sea (Fig. 1(c, f)).

Similar to the temperature responses, the change in annual mean precipitation remains insignificant in most of East Asia, except for the increased precipitation in the Japan Sea and decreased precipitation along southern coastal China (Fig. 2(a, d)). Compared with the annual precipitation changes, the adjustments in seasonal precipitation are more complex. Significant changes occur in winter in the Japan Sea, with a substantial increase of approximately 20 mm/month. Conversely, winter precipitation changes in the other regions are small (within the range of less than 3 mm/month). This reduces slightly over the South China Sea (Fig. 2(b, e)). During the summer, a drying anomaly is evident in southern China, accompanied by increased precipitation in northern China, with amplitudes of approximately 10 mm/month (Fig. 2(c, f)).

The changes in low-level wind fields (Fig. 3), combined with the spatial distribution of water vapor (Fig. 4), contribute to the simulated precipitation patterns. In winter, cyclonic anomalies appear over the Japan Sea, indicating a weakening of the western Pacific high and a strengthening of the East Asian trough. Along the western side of these anomalies, anomalous northeasterlies flow over northern China, while anomalous northwesterlies flow over southern China (Fig. 3(b, e)). Such circulation anomalies induce moisture convergence over the Japan Sea and subsequent transport from north to south over eastern China, leading to a slight increase in winter precipitation in northern China but a notable reduction in precipitation over southern China and the South China Sea (Figs. 2(b, e) and 4(b, e)). The mid–high latitude inland regions exhibit an easterly or northeasterly anomaly (Fig. 3(b, e)), indicating a weakening of the westerly jet stream. The significant anomalous areas are associated with a slight decrease in precipitation (Fig. 2(b, e)). In summer, the rise in sea level leads to a strengthening of the western Pacific high and weakening of the monsoon circulation (Fig. 3(c, f)), resulting in increased moisture transport from the Pacific Ocean to

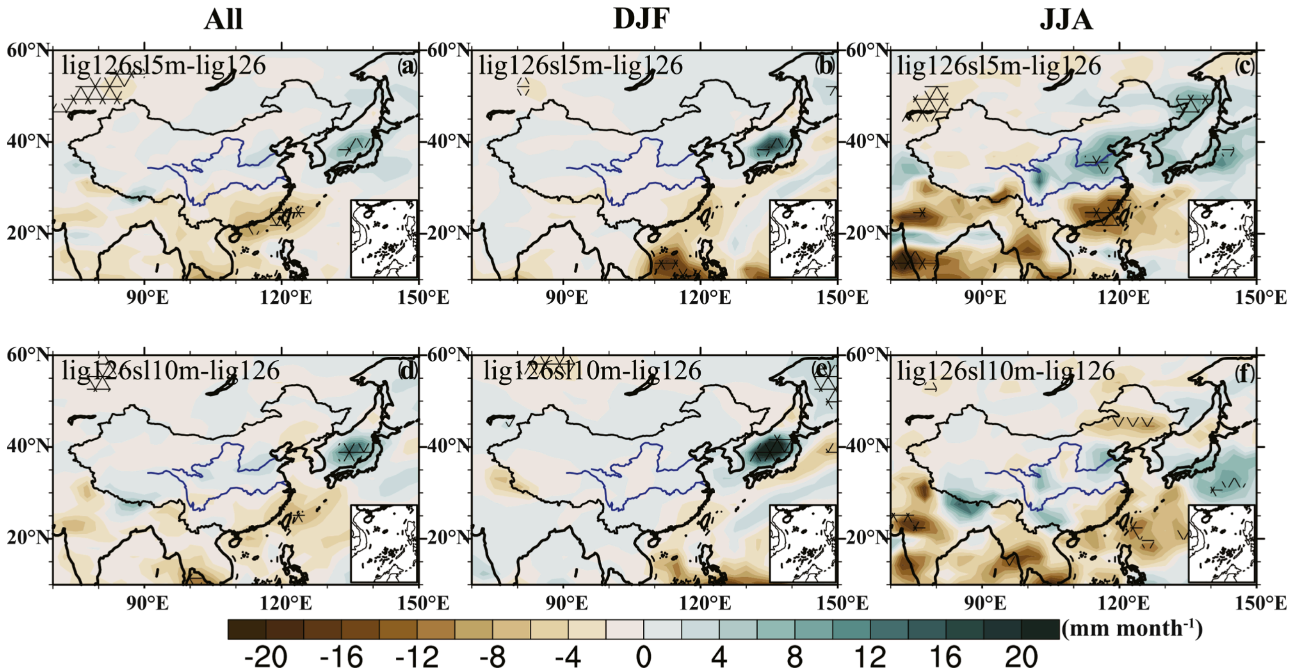

Fig. 2. Monthly precipitation changes due to GMSL rise in interglacial sensitivity experiments: (a) comparison between the lig126sl5m and lig126 experiments in the response of monthly precipitation (units: mm/month) for the whole year; (b, c) as in (a) but in winter (DJF) and summer (JJA), respectively; (d–f) as in (a–c) but the sea-level uplifts are 10 m. The gridded area passed the 0.05 significance *t*-test.

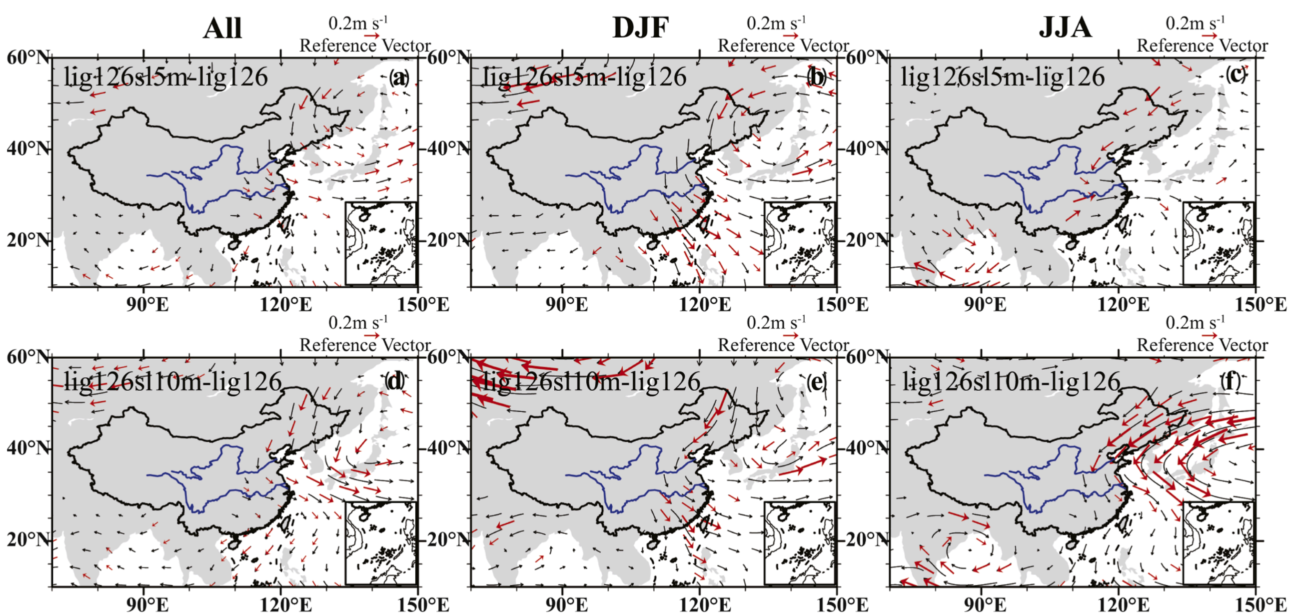

Fig. 3. Monthly wind speed changes at 850 hPa due to GMSL rise in interglacial sensitivity experiments: (a) comparison between the lig126sl5m and lig126 experiments in the response of monthly wind speed (units: m s^{-1}) for the whole year; (b, c) as in (a) but in winter (DJF) and summer (JJA), respectively; (d–f) as in (a–c) but the sea-level uplifts are 10 m. The red arrows passed the 0.05 significance *t*-test.

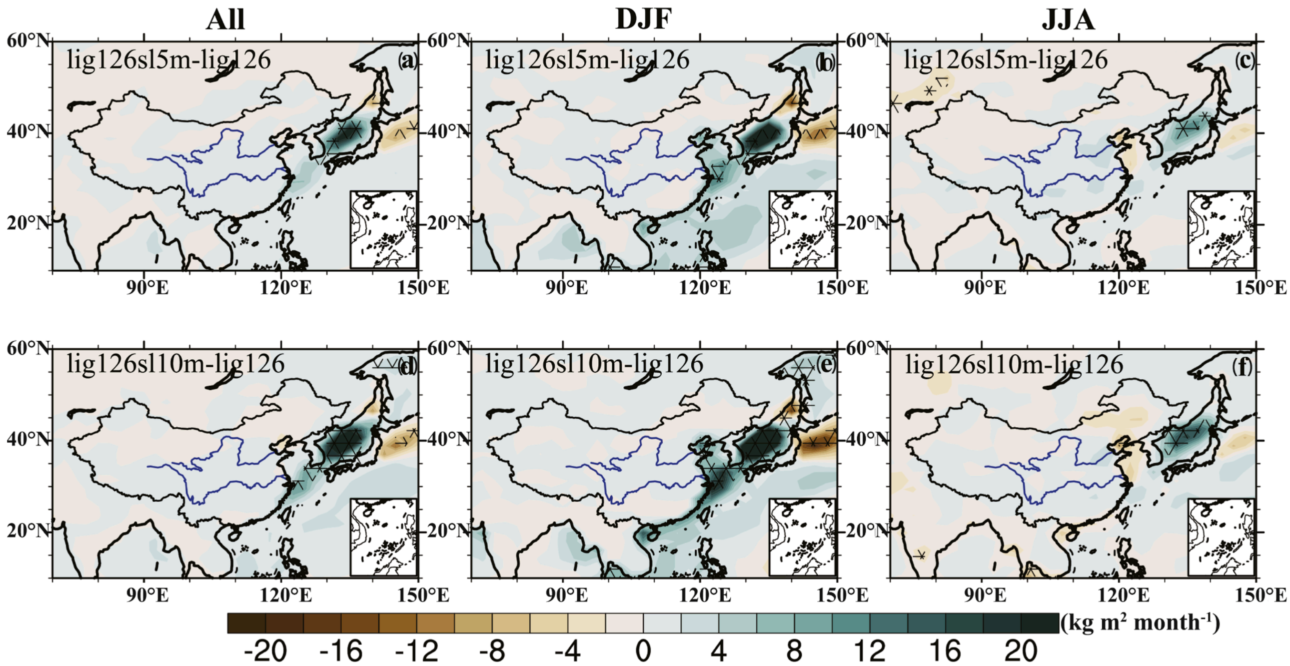

Fig. 4. Monthly surface water flux changes due to GMSL rise in interglacial sensitivity experiments: (a) comparison between the lig126sl5m and lig126 experiments in the response of monthly surface water flux (units: kg m^{-2}/month) for the whole year; (b, c) as in (a) but in winter (DJF) and summer (JJA), respectively; (d–f) as in (a–c) but the sea-level uplifts are 10 m. The gridded area passed the 0.05 significance *t*-test.

northern China, whereas the moisture flux to southern China decreases.

But do these changes help rectify the model–data mismatch? Comparison between the lig126 and piControl experiments shows a winter cooling and summer warming of up to 5 °C (Jiang et al., 2022), but a general cooling in the annual mean (Fig. 5(a)). In terms of annual precipitation, the lig126 experiment shows that western China is wetter, whereas eastern China is drier, compared to the pre-industrial experiment (Fig. 5(d)). Even when considering high sea-levels in the lig126sl5m and lig126sl10m experiments, the patterns of annual mean temperature and precipitation responses do not change significantly. Compared with the reconstruction records (Table 1) collected in a previous study (Leng et al., 2019), the simulated annual temperature and precipitation still exhibit a remarkable mismatch (Fig. 5(b, c, e, f)). This comparison demonstrates that the direct effect of sea-level rise is insufficient to explain the model–data mismatch in China during the LIG.

4. Discussion and conclusions

In summary, the lig126sl5m and lig126sl10m experiments demonstrate a slight increase in annual mean SAT in China, particularly in the Japan Sea and eastern coastal regions. The changes in seasonal temperature and precipitation also align with the overall patterns observed in the annual mean. However, these simulated results still exhibit a notable mismatch when compared with reconstruction records, indicating the need for further investigation and refinement in the model simulations.

Although the consideration of GMSL rise has successfully reduced the model–data mismatch in the Southern Hemisphere (Zhang et al., 2023), its direct effect on reducing the mismatch in East Asia is challenging. The discrepancy is likely due to uncertainties in both reconstructions and simulations.

Some studies suggest that the temperature proxies used for the LIG may exhibit a bias towards the warm season, reflecting summer temperatures rather than annual mean temperatures. This bias can lead to generally warmer reconstruction results (Bakker and Renssen, 2014). In addition, climate proxies often capture combined climate signals, making extracting a single climate signal (for example, pure precipitation) challenging (e.g., Miao et al., 2015; Thomas et al., 2016). Finally, uncertainties in dating techniques and differences in methods for analyzing proxy indicators (Jiang et al., 2012) also contribute to the overall uncertainties in reconstructions.

On the simulation side, our experiments remain idealized by uniformly lifting sea-level spatially (Zhang et al., 2023). In reality, a GMSL rise triggers numerous complex processes that cannot be fully captured in climate models. For instance, the fixed vegetation and ice cover conditions in our experiments may have biased the simulated temperature, surface evaporation, and water budget (Capron et al., 2014; Otto-Bliesner et al., 2020). A GMSL rise can potentially induce changes in vegetation feedback, although the extent of this effect remains uncertain. Cloud feedback in simulations also introduces uncertainty (Stephens, 2005; Liu et al., 2014), as it is not yet clearly understood how a GMSL rise influences cloud feedback. The coarse horizontal resolution may not capture the localized environmental influences on East Asian precipitation (Jiang et al., 2022). Given that GMSL rise is a slow feedback process, future investigations must delve deeper into the various slow feedback processes related to sea-level rise. Additionally, the potential influence of the calendar effect should be considered, though it is small.

Future research should focus on improving climate models by incorporating dynamic bathymetry, topography changes, and feedback mechanisms related to relative sea-level changes to address these issues and reduce the model–data mismatch. Meanwhile, more comprehensive and high-resolution reconstructions, using multiple proxies and reducing dating uncertainties, are also crucial. All these new approaches will enhance our understanding of the LIG and the future warmer climate.

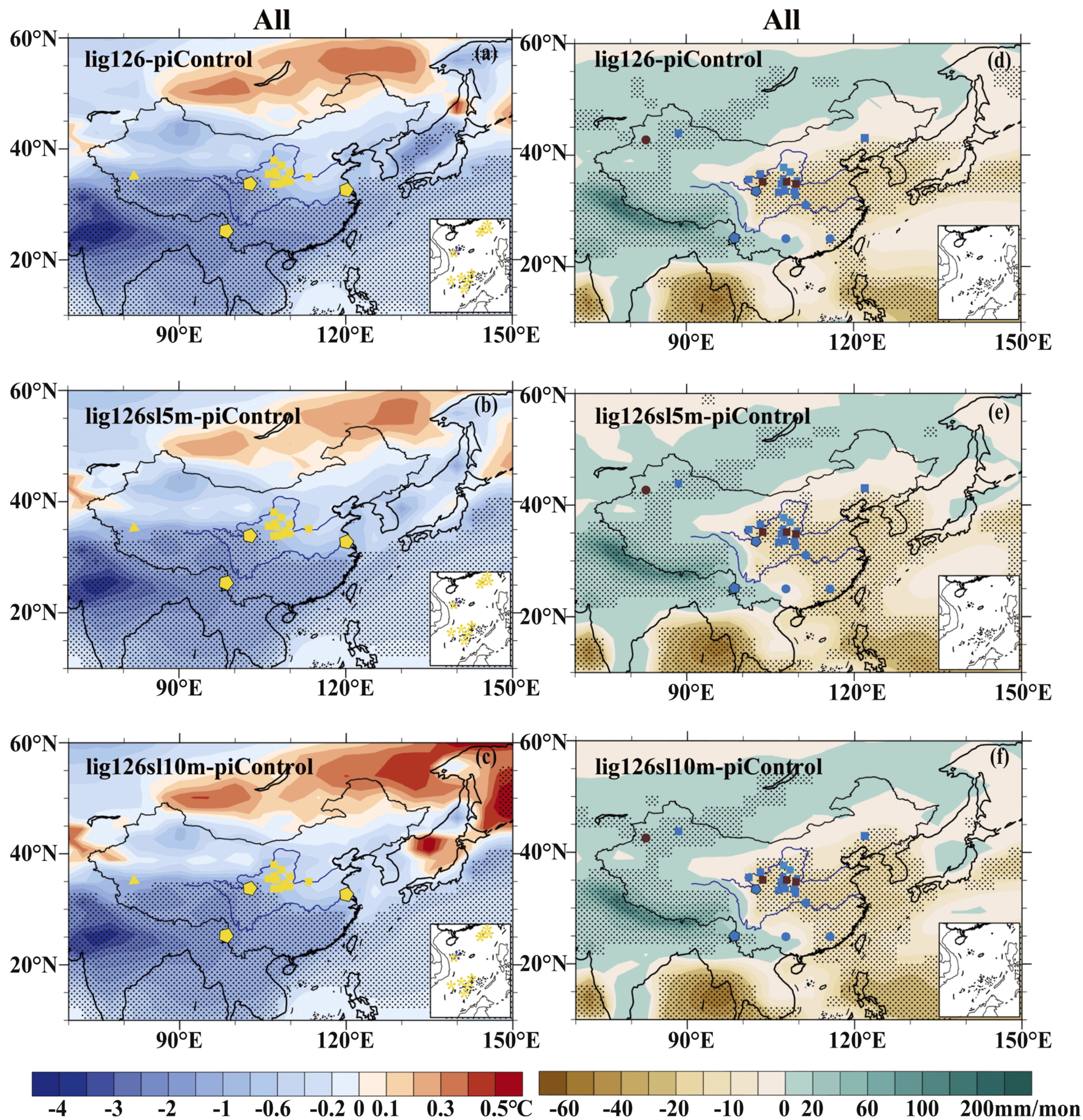

Fig. 5. Monthly temperature and precipitation changes across the whole year due to GMSL rise and geological records: (a) comparison between the lig126 and piControl experiments in the response of monthly temperature (units: ℃) for the whole year; (b, c) as in (a) but the sea-level uplifts are 5 m and 10 m, respectively; (d–f) as in (a–c) but for monthly precipitation change (units: mm/month). Only the changes that are significant at the 0.05 level are shown. Triangles, ice cores; rectangles, loess deposits; circles, stalagmites; pentagons; lake sediment; asterisks, deep sea sediment; yellow/blue (blue/brown) indicates +/– in temperature (precipitation).

Funding

This study was jointly supported by the National Natural Science Foundation of China [grants numbers 42125502, 42230208, and 42172039].

References

Bakker, P., Renssen, H., 2014. Last Interglacial model–data mismatch of thermal maximum temperatures partially explained. Clim. Past 10 (4), 1633–1644. https://doi.org/10.5194/cp-10-1633-2014.

Beck, J.W., Zhou, W., Li, C., Wu, Z., White, L., Xian, F., Kong, X., An, Z., 2018. A 550,000-year record of East Asian monsoon rainfall from 10Be in loess. Science 360 (6391), 877. https://doi.org/10.1126/science.aam5825.

Berger, A., Loutre, M.F., 1991. Insolation values for the climate of the last 10 million years. Quat. Sci. Rev. 10 (4), 297–317. https://doi.org/10.1016/0277-3791(91)90033-Q.

Capron, E., Govin, A., Stone, E.J., Masson-Delmotte, V., Mulitza, S., Otto-Bliesner, B., Rasmussen, T.L., Sime, L.C., Waelbroeck, C., Wolff, E.W., 2014. Temporal and spatial structure of multi-millennial temperature changes at high latitudes during the Last Interglacial. Quat. Sci. Rev. 103, 116–133. https://doi.org/10.1016/j.quascirev.2014.08.018.

Cheng, H., Edwards, R.L., Sinha, A., Spötl, C., Yi, L., Chen, S., Kelly, M., et al., 2016. The Asian monsoon over the past 640,000 years and ice age terminations. Nature 534 (7609), 640. https://doi.org/10.1038/nature18591.

Chen, Y., Chen, J., Liu, L., Ji, J., Zhang, J., 2003. The Rb/Sr record of the Loess Plateau and the temporal and spatial changes of the summer monsoon in the recent 130,000 years. Sci. China 33 (6), 513–519. https://doi.org/10.3969/j.issn.1674-7240.2003.06.003.

Church, J.A., White, N.J., Coleman, R., Lambeck, K., Mitrovica, J.X., 2004. Estimates of the regional distribution of sea level rise over the 1950-2000 period. J. Clim. 17 (13), 2609–2625. doi:10.1175/1520-0442(2004)017<2609:EOTRDO>2.0.CO;2.

Di Nezio, P.N., Timmermann, A., Tierney, J.E., Jin, F., Otto-Bliesner, B., Rosenbloom, N., Mapes, B, et al., 2016. The climate response of the Indo-Pacific warm pool to glacial sea level. Paleoceanography 31 (6), 866–894. https://doi.org/10.1002/2015PA002890.

Du, S., Li, B., Li, Z., Chen, M., Zhang, D.D., Xiang, R., Niu, D., Si, Y., 2016. East Asian monsoon precipitation and paleoclimate records since the last interglacial period in the Bohai Sea coastal zone, China. Terr. Atmos. Ocean. Sci. 27 (6), 825–836. https://doi.org/10.3319/TAO.2016.02.04.01(TT).

Farnsworth, A., Lunt, D.J., O'Brien, C.L., Foster, G.L., Inglis, G.N., Markwick, P., Pancost, R.D., Robinson, S.A., 2019. Climate sensitivity on geological timescales controlled by nonlinear feedbacks and ocean circulation. Geophys. Res. Lett. 46 (16), 9880–9889. https://doi.org/10.1029/2019GL083574.

Fox-Kemper, B., Hewitt, H.T., Xiao, C, Aðalgeirsdóttir, G., Drijfhout, S.S., Edwards, T.L., Golledge, N.R., et al., 2021. Ocean, cryosphere and sea level change. In: Masson-Delmotte, V., Zhai, P., Pirani, A., Connors, S.L., Péan, C., Berger, S., Caud, N (Eds.), et al., Climate Change 2021: The Physical Science Basis Contribution of Working Group I to the Sixth Assessment Report of the Intergovernmental Panel on Climate Change. Cambridge University Press, Cambridge, pp. 1211–1361. https://doi.org/10.1017/9781009157896.011.

Gent, P.R., Danabasoglu, G., Donner, L.J., Holland, M.M., Hunke, E.C., Jayne, S.R., Lawrence, D.M, et al., 2011. The community climate system model version 4. J. Clim. 24 (19), 4973–4991. https://doi.org/10.1175/2011JCLI4083.1.

Guo, C., Bentsen, M., Bethke, I., Ilicak, M., Tjiputra, J., Toniazzo, T., Schwinger, J., Otterå, O.H., 2019. Description and evaluation of NorESM1-F: A fast version of the Norwegian Earth System Model (NorESM). Geosci. Model Dev. 12 (1), 343–362. https://doi.org/10.5194/gmd-12-343-2019.

Guo, P., 2004. Ancient Vegetation and Paleoclimatic Records Since the Late Pleistocene in Xinhua, Subei Basin. Msc Thesis. Nanjing Normal University, pp. 1–39. https://doi.org/10.7666/d.y642656.

Guo, Z., Fedoroff, N., Liu, D., 1993. Paleosol evidence of difference of climates between Holocene and the last interglacial. Quat. Sci. (1),, 41–55. http://www.dsjyj.com.cn/article/id/dsjyj_9856.

He, J., Zhao, M., Li, L., Wang, P., Ge, H., 2008. Surface seawater temperature and terrestrial biomarker records of the sedimentary column of MD05-2904 in the northern South China Sea since 260,000 years. Chin. Sci. Bull. 53 (11), 1324. https://doi.org/10.1360/csb2008-53-11-1324.

Hoffman, J.S., Clark, P.U., Parnell, A.C., He, F., 2017. Regional and global sea-surface temperatures during the last interglaciation. Science 355 (6322), 276–279. https://doi.org/10.1126/science.aai8464.

Hu, A., Meehl, G.A., Otto-Bliesner, B.L., Waelbroeck, C., Han, W., Loutre, M., Lambeck, K., Mitrovica, J.X., Rosenbloom, N., 2010. Influence of Bering Strait flow and North Atlantic circulation on glacial sea-level changes. Nat. Geosci. 3 (2), 118–121. https://doi.org/10.1038/ngeo729.

Hu, C., Wang, Y., Li, A., Liao, J., Xie, S., 2015. Comparison of stalagmite records of precipitation changes in eastern monsoon region and northwest arid region of China. Earth Sci. J. China Univ. Geosci. 40 (1), 268–274.

Jiang, D., Lang, X., Tian, Z., Wang, T., 2012. Considerable model–data mismatch in temperature over China during the mid-Holocene: results of PMIP simulations. J. Clim. 25 (12), 4135–4153. https://doi.org/10.1175/JCLI-D-11-00231.1.

Jiang, N., Yan, Q., Wang, H., 2022. General characteristics of climate change over China and associated dynamic mechanisms during the Last Interglacial based on PMIP4 simulations. Global Planet. Chang. 208, 103700 https://doi.org/10.1016/j.gloplacha.2021.103700.

Jiang, X., Wang, Y., Kong, X., Chen, S., Li, M., Chen, H., 2008. Climate variability in Shennongjia during the last interglacial inferred from a high-resolution stalagmite record. Acta Sedimentol. Sin. 26 (1), 139–144. http://www.cjxb.ac.cn/article/id/1089.

Jin, H., Li, M., Su, Z., Dong, G., Zhao, H., 2005. Geochemical features of a profile in Salawusu River Valley and their response to global climate changes since 220 ka BP. J. Glaciol. Geocryol. 27 (6), 861–868. https://doi.org/10.7522/j.issn.1000-0240.2005.0128.

Leng, S., Zhang, Z., Dai, G., 2019. Two climate models simulation of MIS5 climate in China. Quat. Sci. 39 (6), 1357–1371. https://doi.org/10.11928/j.issn.1001-7410.2019.06.04.

Li, L., Wang, H., Li, J.R., Zhao, M., Wang, P., 2009. Changes in sea surface temperature in western South China Sea over the past 450 ka. Chin. Sci. Bull. 54 (18), 3335–3343. https://doi.org/10.1007/s11434-009-0083-9.

Liang, D., Li, L., Li, Q., Wang, H., 2015. Hydroclimate implications of thermocline variability in the southern South China Sea over the past 180,000 yr. Quat. Res. 83 (2), 370–377. https://doi.org/10.1016/j.yqres.2014.12.003.

Liu, Z., Pan, B., Wu, G., Guan, Q., 2000. Preliminary study on the summer monsoon change in the desert marginal area of Northwestern China since the last interglacial period. J. Desert Res. 20 (4), 375–377. https://doi.org/10.3321/j.issn:1000-694X.2000.04.006.

Liu, Z., Zhu, J., Rosenthal, Y., Zhang, X., Otto-Bliesner, B.L., Timmermann, A., Smith, R. S, et al., 2014. The Holocene temperature conundrum. Proc. Natl. Acad. Sci. 111 (34), E3501–E3505. https://doi.org/10.1073/pnas.1407229111.

Lu, H., Wu, N., Liu, K., Jiang, H., Liu, D., 2007. Phytoliths as quantitative indicators for the reconstruction of past environmental conditions in China II: palaeoenvironmental reconstruction in the Loess Plateau. Quat. Sci. Rev. 26 (5-6), 759–772. https://doi.org/10.1016/j.quascirev.2006.10.006.

Lü, H., Wu, N., Liu, D., Han, J., Qin, X., Sun, X., Wang, Y., 1996. Seasonal climate change of Baoji loess plants silica since 150 ka. Sci. China 26 (2), 131–136. https://www.sciengine.com/Sci%20Sin%20Terrae-D/doi/10.1360/zd1996-26-2-131.

Lü, L., 1999. High-Resolution Climate Change in the Western Part of the Loess Plateau and Qinghai-Tibet Plateau since 150,000. Msc Thesis. Lanzhou University, pp. 1–53. https://doi.org/10.7666/d.Y305437.

Miao, Y., Zhang, P., Lu, S., Wu, X., Li, L., Chen, H., Li, X., Miao, Q., Feng, W., Ou, J., 2015. Late quaternary pollen records from the Yangtze River Delta, East China, and its implications for the Asian monsoon evolution. Arab. J. Geosci. 8, 7845–7854. https://doi.org/10.1007/s12517-015-1777-8.

Ning, Y., Liu, W., An, Z., 2008. A 130-ka reconstruction of precipitation on the Chinese Loess Plateau from organic carbon isotopes. Palaeogeogr. Palaeoclimatol. Palaeoecol. 270 (1-2), 59–63. https://doi.org/10.1016/j.palaeo.2008.08.015.

Oppo, D.W., Sun, Y., 2005. Amplitude and timing of sea-surface temperature change in the northern South China Sea: Dynamical link to the East Asian monsoon. Geology 33 (10), 785–788. https://doi.org/10.1130/G21867.1.

Otto-Bliesner, B.L., Brady, E.C., Tomas, R.A., Albani, S., Bartlein, P.J., Mahowald, N.M., Shafer, S.L, et al., 2020. A comparison of the CMIP6 midHolocene and lig127k simulations in CESM2. Paleoceanogr. Paleoclimatol. 35 (11), e2020PA003957 https://doi.org/10.1029/2020PA003957.

Otto-Bliesner, B.L., Brady, E.C., Zhao, A., Brierley, C.M., Axford, Y., Capron, E., Govin, A, et al., 2021. Large-scale features of Last Interglacial climate: Results from evaluating the lig127k simulations for the Coupled Model Intercomparison Project (CMIP6)–Paleoclimate Modeling Intercomparison Project (PMIP4). Clim. Past 17 (1), 63–94. https://doi.org/10.5194/cp-17-63-2021.

Past Interglacials Working Group of PAGES, 2016. Interglacials of the last 800,000 years. Rev. Geophys. 54 (1), 162–219. https://doi.org/10.1002/2015RG000482.

Pedersen, R.A., Langen, P.L., Vinther, B.M., 2017. The last interglacial climate: comparing direct and indirect impacts of insolation changes. Clim. Dyn. 48 (9), 3391–3407. https://doi.org/10.1007/s00382-016-3274-5.

Pelejero, C., Grimalt, J.O., Heilig, S., Kienast, M., Wang, L., 1999a. High-resolution UK37 temperature reconstructions in the South China Sea over the past 220 kyr. Paleoceanography 14 (2), 224–231. https://doi.org/10.1029/1998PA900015.

Pelejero, C., Grimalt, J.O., Sarthein, M., Wang, L., Flores, J., 1999b. Molecular biomarker record of sea surface temperature and climatic change in the South China Sea during the last 140,000 years. Mar. Geol. 156 (1-4), 109–121. https://doi.org/10.1016/S0025-3227(98)00175-3.

Petersen, F., Martínez-García, A., Zhou, B., Beets, C.J., Prins, M.A., Zheng, H., Eglinton, T.I., 2014. Molecular records of continental air temperature and monsoon precipitation variability in East Asia spanning the past 130,000 years. Quat. Sci. Rev. 83, 76–82. https://doi.org/10.1016/j.quascirev.2013.11.001.

Petit, J.R., Raynaud, D., Basile, I., Chappellaz, J., Davisk, M., Ritz, C., Delmotte, M, et al., 1999. Climate and atmospheric history of the past 420,000 years from the Vostok ice core, Antarctica. Nature 399 (6735), 429–436. https://doi.org/10.1038/20859.

Qin, J., Yuan, D., Lin, Y., Zhang, M., 2001. Records of high-resolution climate events from stalagmites since 160,000 a BP in Guangxi and Guizhou provinces, China. Earth Sci. Front. 8 (1), 99–105. https://doi.org/10.3321/j.issn:1005-2321.2001.01.013.

Qiu, X., Li, T., Nan, Q., Gong, H., 2014. Carbon isotope minimum events in the northern margin of western Pacific Warm Pools since during the past 150 ka. Mar. Sci. 38 (11), 116–121. http://qdhys.ijournal.cn/hykx/ch/reader/view_abstract.aspx?file_no=20141117&flag=1.

Richter, K., Meyssignac, B., Slangen, A.B., Melet, A., Church, J.A., Fettweis, X., Marzeion, B, et al., 2020. Detecting a forced signal in satellite-era sea-level change. Environ. Res. Lett. 15 (9), 094079 https://doi.org/10.1088/1748-9326/ab986e.

Shen, C., Tang, L., Wang, S., Li, C., Liao, G., 2005. RM pore spore-pollen record and its chronostratigraphical sequence in the Zuoqiuping Basin. Chin. Sci. Bull. 50 (3), 246–254. doi:10.3321/j.issn:0023-074X.2005.03.009.

Siegenthaler, U., Stocker, T.F., Monnin, E., Luthi, D., Schwander, J., Stauffer, B., Raynaud, D, et al., 2005. Stable carbon cycle climate relationship during the Late Pleistocene. Science 310 (5752), 1313–1317. https://doi.org/10.1126/science.1120130.

Stephens, G.L., 2005. Cloud feedbacks in the climate system: a critical review. J. Clim. 18 (2), 237–273. https://doi.org/10.1175/JCLI-3243.1.

Su, X., Liu, C., Beaufort, L., Tian, J., Huang, E., 2013. Late quaternary coccolith records in the South China Sea and East Asian monsoon dynamics. Global Planet. Change 111 (12), 88–96. https://doi.org/10.1016/j.gloplacha.2013.08.016.

Tang, C., Yang, H., Pancost, R.D., Griffiths, M.L., Xiao, G., Dang, X., Xie, S., 2017. Tropical and high-latitude forcing of enhanced megadroughts in Northern China during the last four terminations. Earth Planet. Sci. Lett. 479, 98–107. https://doi.org/10.1016/j.epsl.2017.09.012.

Thomas, E.K., Clemens, S.C., Sun, Y., Prell, W.L., Huang, Y., Gao, L., Loomis, S., Chen, G., Liu, Z., 2016. Heterodynes dominate precipitation isotopes in the East Asian monsoon region, reflecting interaction of multiple climate factors. Earth Planet. Sci. Lett. 455, 196–206. https://doi.org/10.1016/j.epsl.2016.09.044.

Turney, C.S., Jones, R.T., McKay, N.P., Van Sebille, E., Thomas, Z.A., Hillenbrand, C.D., Fogwill, C.J., 2020. A global mean sea surface temperature dataset for the Last Interglacial (129–116 ka) and contribution of thermal expansion to sea level change. Earth Syst. Sci. Data 12 (4), 3341–3356. https://doi.org/10.5194/essd-12-3341-2020.

Wang, P., Min, Q., Bian, Y., Feng, W., 1986. Planktonic foraminifera on the northern slope of the South China Sea during the past 130,000 years and its paleoceanographic significance. Acta Geol. Sin. 60 (3), 3–13. http://geo.ijournals.cn/dzxb/dzxb/article/abstract/19860319?st=article_issue.

Wang, P., Li, Q., Tian, J., Jian, Z., Liu, C., Li, L., Ma, W., 2014. Long-term cycles in the carbon reservoir of the quaternary ocean: a perspective from the South China Sea. Natl. Sci. Rev. 1 (1), 119–143. https://doi.org/10.1093/nsr/nwt028.

Wen, Q., Diao, G., Jia, R., Sun, J., Zhou, H., 1997. Geochemical records of paleoclimatic changes in the Weihe section since the last interglacial. Chin. Geogr. Sci. 7 (1), 39–46. https://doi.org/10.1007/s11769-997-0070-5.

Wen, Y., 2007. Sedimentary Records of the Tengchong Beihai Wetland Since 150 ka and the Evolution of the South Asian Summer Monsoon. Msc Thesis. China University of Geosciences(Beijing), pp. 1–60. http://cdmd.cnki.com.cn/Article/CDMD-11415-2007067153.htm.

Wen, Y., 2015. Preliminary Study on Climate Change Since the Last Interglacial Perion Recorded in the Northern Loess of Tianshan Mountains. Msc Thesis. Lanzhou University. https://kns.cnki.net/kcms2/article/abstract?v=3uoqIhG8C475KOm_zrgu4lQARvep2SAkVtq-vp-8QbjqyhlE-4l1Ysg0QqAslVVBZreiDI6Lv1L6wGOBmCnFA5ustq9RG31F&uniplatform=NZKPT.

Wu, G., Yao, T., Thompson, L.G., Li, Z., 2004. The comparison between the records of particles in the Guliya Ice core and the polar ice cores since the Last Interglacial. Chin. Sci. Bull. 49 (5), 475–479. doi:10.3321/j.issn:0023-074X.2004.05.013.

Wu, J., Wang, S., Shi, Y., Jie, L., 2000. Quantitative study of paleotemperature of oxygen isotope records since 200 ka in Zuoqiuping Basin. Sci. China 30 (1), 73–80. https://www.sciengine.com/Sci%20Sin%20Terrae-D/doi/10.1360/zd2000-30-1-73.

Xue, B., Wang, S., Wu, Y., Xia, W., Wu, J., Qian, J., Hu, S., Wang, Y., 1999. Palaeoenvironmental reconstruction of Zuoqiuping Basin of eastern Tibetan Plateau during the past 140 ka. J. Lake Sci. 11 (3), 206–212. https://doi.org/10.18307/1999.0303.

Yamamoto, M., Sai, H., Chen, M.T., Zhao, M., 2013. The East Asian winter monsoon variability in response to precession during the past 150,000 years. Clim. Past 9 (6), 2777–2788. https://doi.org/10.5194/cp-9-2777-2013.

Yao, T., Shi, Y., Qin, D., Jiao, K., Yang, Z., Tian, L., Thompson, L.G., Mosley-Thomp, E., 1997. Research of climate change recorded in Guliya Ice Cores since the last interglacial. Sci. China 27 (5), 447–452. https://www.sciengine.com/Sci%20Sin%20Terrae-D/doi/10.1360/zd1997-27-5-447.

Zhang, H., 2013. Research on Sedimentary Environment and Paleoclimate Changes Since 130 Thousand Years Stage in Linfen Basin. Msc Thesis. Shanxi Normal University, pp. 1–33. https://doi.org/10.7666/d.Y2307159.

Zhang, Z., Jansen, E., Sobolowski, S.P., Otterå, O.H., Ramstein, G., Guo, C., Nummelin, A, et al., 2023. Atmospheric and oceanic circulation altered by global mean sea-level rise. Nat. Geosci. 16, 321–327. https://doi.org/10.1038/s41561-023-01153-y.

Zhao, J., Li, D., Lu, H., Zhang, X., Li, Y., Wang, D., 2004. The variation of CaCO3 content in four profiles from the north of China and the reconstructed paleo-precipitations. Mar. Geol. Quat. Geol. 24 (3), 117–122 (In Chinese).

Zhao, M., Huang, C.Y., Wang, C.C., Wei, G., 2006. Amillennial-scale U37K' sea-surface temperature record from the South China Sea (8°N) over the last 150 kyr: monsoon and sea-level influence. Palaeogeogr. Palaeoclimatol. Palaeoecol. 236 (1), 39–55. https://doi.org/10.1016/j.palaeo.2005.11.033.

Zhou, W., Xian, F., Du, Y., Kong, X., Wu, Z., 2014. The last 130 ka precipitation reconstruction from Chinese loess 10Be. J. Geophys. Res. 119 (1), 191–197. https://doi.org/10.1002/2013JB010296.